Proceedings of the
International Conference on Mechanical Engineering and Renewable Energy 2015
(ICMERE2015) 26 – 29 November, 2015, Chittagong, Bangladesh

ICMERE2015-PI-273

PERFORMANCE TEST OF NACA 2412 AIRFOIL

Rashed Ahammad[1,*], Md. Kamrul Hasan[2], M. Rahman[3] and M. Chakraborty[4]

[1-4]Student, Department of Mechanical Engineering, CUET, Bangladesh.
[1,*]rashed3434@gmail.com, [2]kamrul05cuet@gmail.com, [3]mmredge@gmail.com, [4]mcb.me72@gmail.com

Abstract- *Computational Fluid Dynamics gives us the opportunity to reduce the cost, time and difficulties of experiments. But only simulation cannot give the total picture. Simulation works only with standard parameters, but in real world results may change. Key parameters that determines the performance of an airfoil are pressure distribution around the foil surface, lift coefficient, drag coefficient, lift to drag ratio and pressure coefficient. This project aims to analyze the performance of an airfoil and compare with experimental results. NACA 2412 airfoil was used in this project for its geometrical simplicity and aerodynamic stability. The fluid flow over NACA 2412 was analyzed both for computer model via simulation and experimental model via wind tunnel. It was observed that both lift and drag force were increasing up to angle 38°. But lift to drag ratio was decreasing after 6°. The stall angle was 38° at 4.3 m/s air speed.*

Keywords: Airfoil, Performance Test, Pressure Distribution, Flow Simulation, Lift to Drag Ratio.

1. INTRODUCTION

Performance test is very important in case of an airfoil. After making it possible to have aircraft, people thought about the efficiency. To improve the efficiency they performed many experiments on various components of aircraft. They tried to reduce its weight, they improved quality of fuel and also they thought about the optimum design of aircraft. Precise shape of airfoil (the cross section of wing) is one of the most important considerations for optimum designs of aircraft. The precise shape of airfoil largely carries the performance of an aircraft. Best performance of aircraft means how smoothly it runs, how much comfort people feel; journey by aircraft is how much safe etc. Performance of airfoil depends on lift coefficient, drag coefficient, angle of attack etc. For better performance, the drag coefficients should be less and the lift coefficients should be large. To understand the performance of an aircraft a wind tunnel test is performed by changing the angles of attack to obtain optimization of aircraft (i.e. at which angles of attack lift drag ratio is maximum).The information obtained from this traditional approach of investigation is very much limited and subjected to measurement errors. Moreover, experiments are only possible when a small-scale model or the actual equipment has already been built. An experimental investigation may be very time consuming, dangerous, prohibitively expensive, or impossible for another reason. To overcome these drawbacks people started the computational study of fluid dynamics. Since it builds a 'virtual prototype' of the system or device that we wish to analyze, it makes our work easy and off course with perfection. The software will provide us with images and data, which predict the performance of the design. The airfoil characteristics vary with changing airfoil shape so; this work is related how this changes in shape affects the characteristics. [1]

2. METHODOLOGY

2.1 Airfoil Selection:

The most important task of this study is to select an airfoil on which the analysis will be done. This study will extremely vary from foil to foil. Result that came out from one foil can't be used to predict behavior of another foil. In this project NACA 2412 was selected and scaled schematic of NACA 2412 is shown in fig. 1.The first family of NACA airfoils, developed in the 1930s, was the "four-digit" series, such as NACA 2412 airfoil. [2]

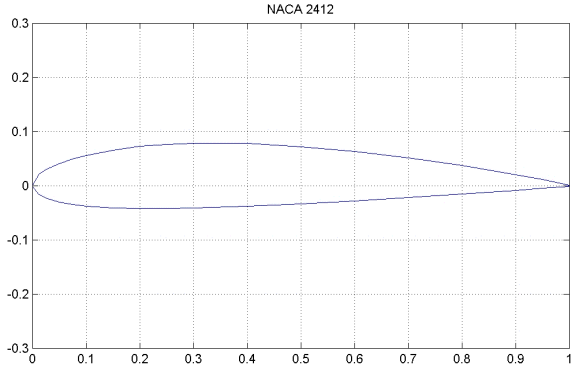

Fig.1: Scaled schematic of NACA 2412 airfoil. [3]

2.2 Computational Study:

The computer simulation was done on SOLIDWORKS Flow Simulation. A model in SolidWorks was created from the data taken from UIUC airfoil database. [4]

2.3 Simulation Setup

The model was built using the 'Curves using XYZ point' function as shown in fig. 2. Chord length was taken 200 mm and span was taken 120 mm for the convenience of using the airfoil in wind tunnel.

(a)

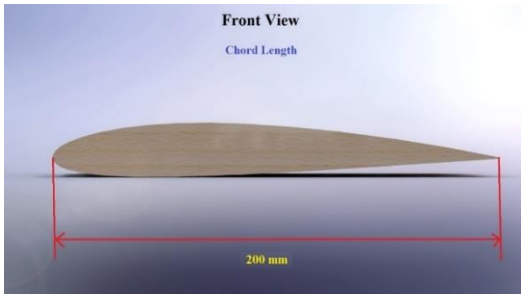

(b)

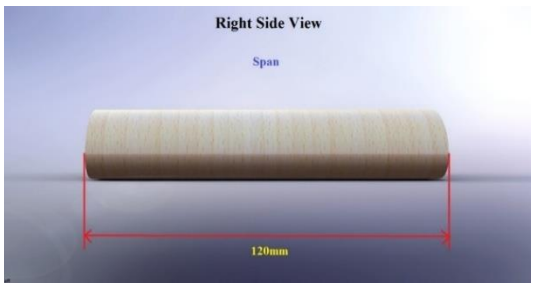

Fig.2: Simulation setup showing the model NACA 2412 airfoil in front view (a) and right side view (b).

The simulation was ran using these parameters:
Fluid was assumed incompressible and the flow was taken laminar.
Fluid: Air
Temperature: 298.2 K
Pressure: 101325 Pa
Air velocity: 4.3 m/s
Air density: 1.15 Kg/m^3
Surface area: 0.024 m^2
Prototype Material: Beech wood (Gamahr)

The SOLIDWORKS Flow Simulation is based upon the use of Cartesian-based meshes and automatic meshing system will create mesh in accordance with the specified minimum gap size, minimum wall thickness, and result resolution level. [5]

2.4 Experimental Setup:

The major elements for experimental setup were a prototype, an open-loop subsonic wind tunnel, a force balance for measuring forces and allows the orientation to be changed during the experiment, pressure taps and multi-tube manometer.

2.5 Prototype:

A prototype (NACA 2412) was built for wind tunnel experiment with the predefined chord length (200mm) and span (120mm). The prototype was built in the workshop not as perfect as wished for. Beech wood (Gamahr) was used as material. The prototype is shown in fig. 3.

Fig.3: Prototype for wind tunnel test.

2.6 Wind Tunnel Testing:

Wind tunnels are an effective tool for understanding relationships between predicted and actual behavior of air foils in laminar flow. The wind tunnel setup used for experiment is shown in fig. 4. Air was sucked through the test section by a large fan located at the rear of the tunnel. A honeycomb was employed in front of the test section to reduce flow turbulence and increase measurement accuracy.

Fig.4: Wind tunnel setup.

2.7. Experimental Steps:

For measuring lift and drag force the prototype was mounted on the force balance which had two degrees of freedom. The force balance in this experiment was used to measure only the axial and normal force. Axial force represents drag force and normal force represents lift force. Air speed was measured using an anemometer.

Lift and drag force for different angle of attack was measured by positioning the prototype using rotation sting. The rotation sting is connected to a shaft equipped with an indexed rotation stage allowing the angle of attack to be varied throughout the test.

The prototype was equipped with 13 surface pressure taps. These pressure taps were connected with the multi-tube manometer via tubes. Pressure was calculated from recorded manometer height measurements using kerosene as working fluid.

3. RESULTS AND DISCUSSION

The goals were set as per objective and the simulation was done for a number of angle of attack starts from 0° to 40°. The figures (from figure 5 (a) to 5 (k)) show velocity distribution for different angle of attack. Turbulent and laminar flow were started to separate by a point of transition or separation point shown in fig 5 (h); as the angle of attack is increased, the portion of the upper airflow that is turbulent also increases. Flow separation occurs when the boundary layer travels far enough against an adverse pressure gradient that the speed of the boundary layer relative to the object falls almost to zero. The fluid flow becomes detached from the surface of the object, and instead takes the forms of eddies and vortices shown in fig. (i), (j), (k). This flow separation can often result in increased drag, particularly pressure drag which is caused by the pressure differential between the fronts and rear surfaces of the object as it travels through the fluid.

(a)

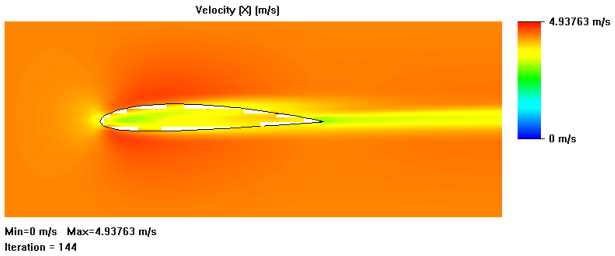

(b)

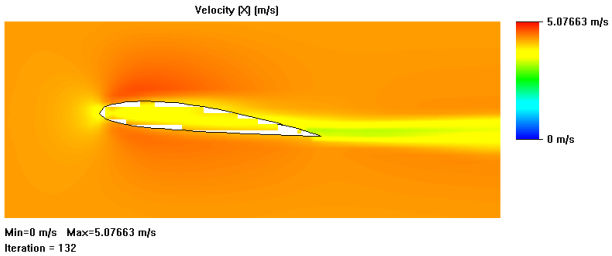

(c)

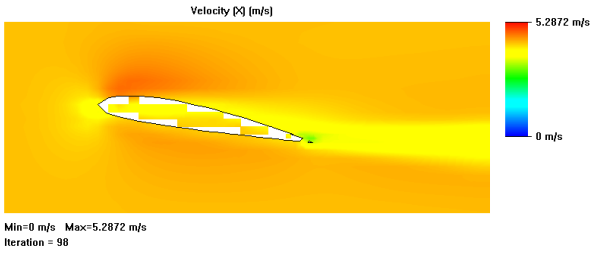

(d)

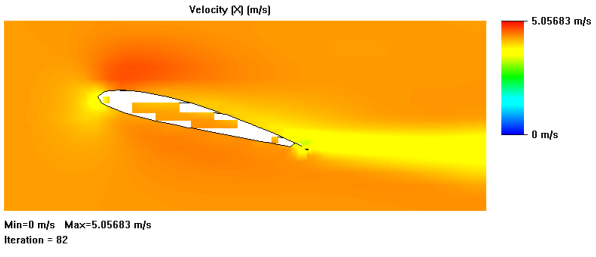

(e)

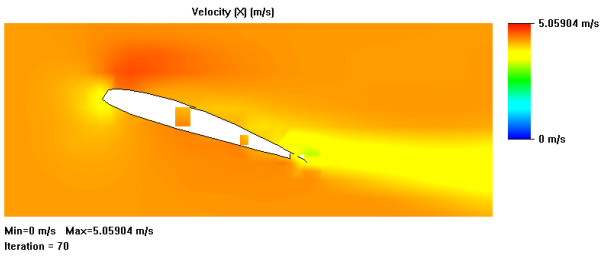

(f)

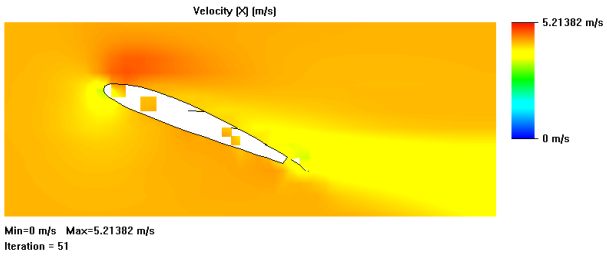

(g)

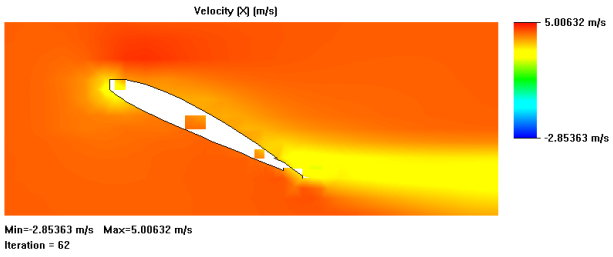

(h)

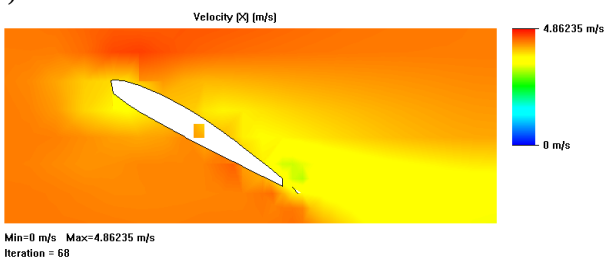

(i)

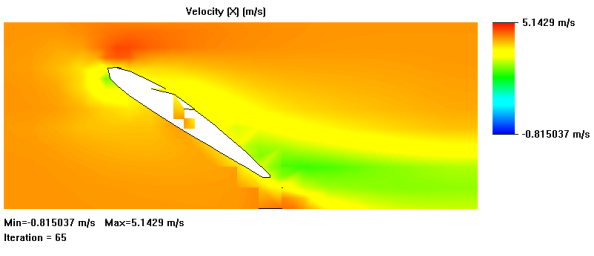

(j)

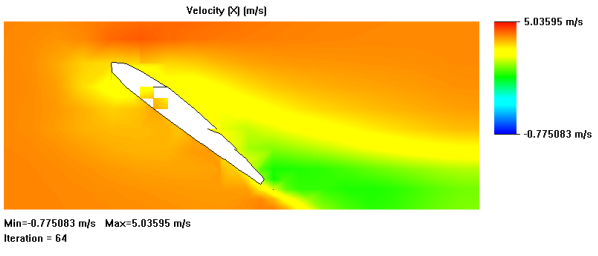

(k)

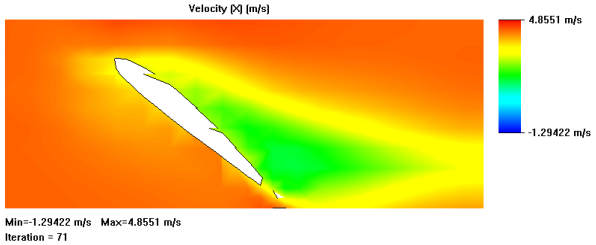

Fig.5: Velocity distribution for angle of attack 0° (a), 6° (b), 10° (c), 14° (d), 18° (e), 22° (f), 26° (g), 30° (h), 34° (i), 38° (j), 40° (k) respectively.

There are many parameters like Reynolds number, thickness ratio, Mach number, angle of attack etc. But here performance of the airfoil was determined by only considering lift and drag force for different angle of attack. From lift and drag force lift coefficient, drag coefficient, lift to drag ratio etc. was measured. Table 1 shows aforementioned terms for different angle of attack.

Table 1: Simulation result.

Angle°	Lift (N)	Drag(N)	L/D	Cl	Cd	Cl/Cd
0	0.0077	0.0031	2.488	0.03	0.012	2.488
6	0.0322	0.00662	4.862	0.126	0.026	4.862
10	0.0543	0.01197	4.539	0.213	0.047	4.539
14	0.0749	0.02162	3.467	0.294	0.085	3.467
18	0.0916	0.03379	2.712	0.359	0.132	2.712
22	0.1209	0.04404	2.746	0.474	0.173	2.746
26	0.1395	0.07358	1.896	0.547	0.288	1.896
30	0.1483	0.0841	1.763	0.581	0.33	1.763
34	0.1553	0.10489	1.481	0.609	0.411	1.481
38	0.159	0.12233	1.3	0.623	0.479	1.3
40	0.1322	0.11968	1.105	0.518	0.469	1.105

In figure 6 it is shown that, for 0° angle of attack lift force is minimum. With gradually increasing angle of attack lift starts to increase. It increases up to angle of attack 38°, and then it begins to fall. In other words stall is initiating. In general, stall angle varies from 15°-22°.But in normal case takeoff and landing speed to a many light airplanes is 20-28 m/s.[6] In this case (Wind Tunnel) it was only 4.3 m/s so the stall angle is 38°. Figure 7 show the behavior of drag force with increasing angle of attack. It also stars from minimum for 0° angle of attack and gradually increasing. In aerodynamics, the lift-to-drag ratio, or L/D ratio, is the amount of lift generated by a wing or vehicle, divided by the aerodynamic drag it creates by moving through the air. Because lift and drag are both aerodynamic forces, the ratio of lift to drag is an indication of the aerodynamic efficiency of the airplane. An airplane has a high L/D ratio if it produces a large amount of lift or a small amount of drag. Under cruise conditions lift is equal to weight. A high lift aircraft can carry a large payload. Under cruise conditions thrust is equal to drag. [7]

Figure 8 represents that with the increase of angle of attack, C_L increases up to 38° then starts to fall. Figure 9 also represents that with the increase of angle of attack C_D increases up to 38° then starts to fall. Figure 10 shows that performance will be maximum at angle of attack 6°.

Pressure distribution along chord length is shown in figure 11. Upper part of the curve shows the pressure distribution of upper surface of the airfoil and lower curve shows lower pressure distribution of the lower surface of the air foil. The area bound by the curve indicates acting lift force.

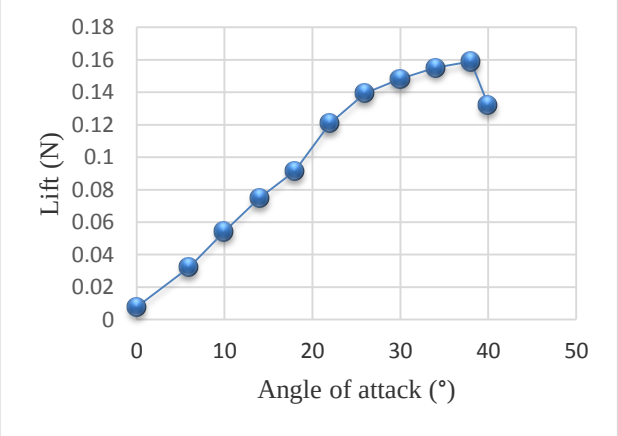

Fig.6: Angle of attack vs. lift.

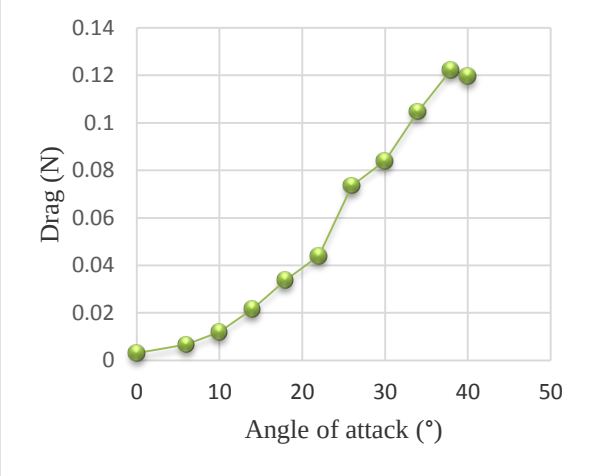

Fig.7: Angle of attack vs. drag.

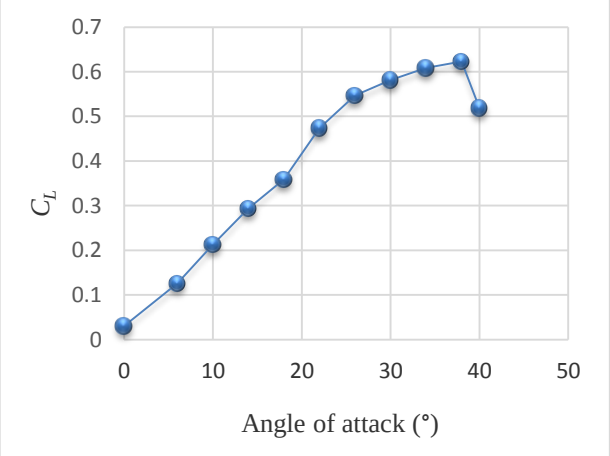

Fig.8: Angle of attack vs. lift coefficient.

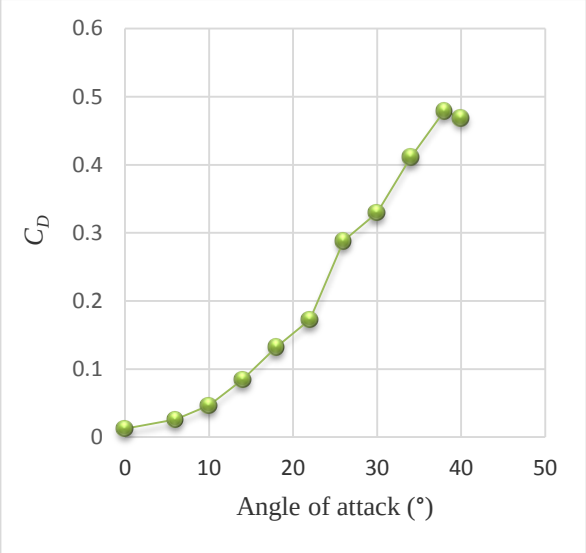

Fig.9: Angle of attack vs. drag coefficient.

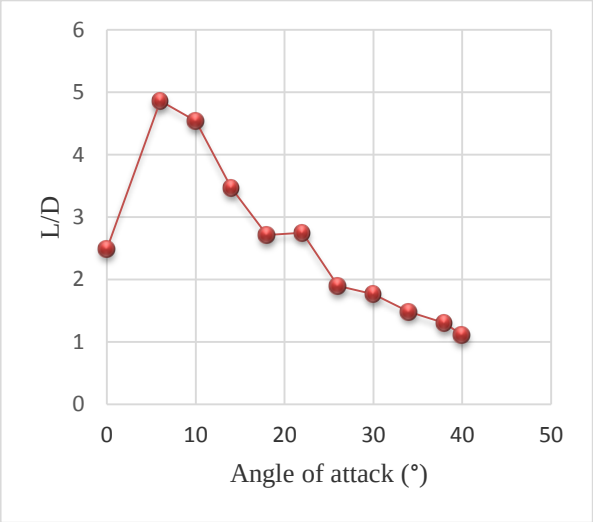

Fig.10: Angle of attack vs. lift to drag ratio.

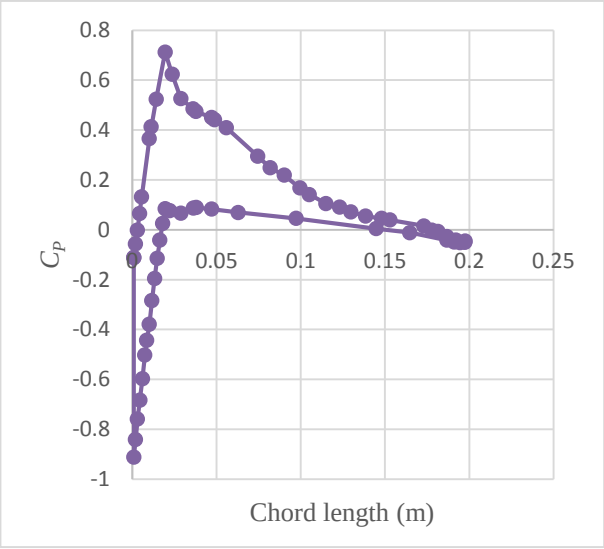

Fig.11: Pressure distribution along chord length of airfoil for angle of attack 10°.

3.1 Experimental Data:

Table 2 and 3 shows both experimental data taken from wind tunnel experiment and difference between the simulation data and experimental data. The difference is huge but there is some explanation.

There are a number of limitations in wind tunnel testing. Wind tunnel testing is generally very expensive and time consuming. In addition, if the object to be tested is too big to fit in the tunnel itself, a very accurate scale model must be produced, and Reynolds numbers must be accurately matched to the expected operating conditions.

The prototype itself was not perfect, though it was designed and built with great care. The prototype was made from wood and machined to desired shape with hand. Therefore, accuracy level drops there much.

Besides, the wind tunnel was old and the data collection technique has become obsolete. Today's wind tunnel use digital force measurement system and pressure sensors for pressure measurement. In most of the case they are coupled with a computer via software. So they can measure data in more accurate level then manual system.

Table 2: Data chart for comparison result (Lift).

Lift force in (N)			
Angle of attack	Experimental result	Simulation result	Error (%)
0	0.062	0.007712852	700%
6	0.242	0.032199505	653%
10	0.42	0.054334291	674%
14	0.48	0.07494392	550%
18	0.66	0.091633972	620%
22	0.91	0.120937114	649%
26	1.01	0.139490453	679%
30	1	0.148302741	575%
34	1.11	0.155334771	612%
38	1.1	0.159015958	589%
40	0.98	0.132215939	643%

Table 3: Data chart for comparison result (Drag).

Drag force in (N)			
Angle of attack	Experimental result	Simulation result	Error (%)
0	0.016	0.003099483	421%
6	0.059	0.0066233	784%
10	0.109	0.011971051	809%
14	0.16	0.021616557	650%
18	0.25	0.033785652	630%
22	0.26	0.044038482	489%
26	0.5	0.0735792	579%
30	0.71	0.084100303	745%
34	0.57	0.104889742	442%
38	1	0.122328239	732%
40	0.97	0.119675677	713%

3.2 Pressure Distribution:

Figure 12 shows pressure distribution along chord length at angle of attack 10°. But it looks quite different from simulation result in Fig 11.

First thing that make the difference is that number of tapping points which determine the accuracy of the curve. In simulation it takes 65 tapping points but in prototype model only 13 tapping points were taken because it was very difficult to make room for so many pressure tubes inside the airfoil. Hence the practical curve for pressure

distribution looks incomplete.

Table 4: Data chart showing C_P along chord length (distance in m).

Distance in m	Cp
0.137	5.32
0.117	5.81
0.097	6.29
0.077	6.53
0.057	7.26
0.037	8.7
0.017	7.24
0.017	4.84
0.037	5.31
0.057	5.45
0.077	5.32
0.097	4.84
0.117	4.8

The pressure measured at a static pressure hole differs slightly from the true static pressure, by an amount which depends on the hole size and shape. The observed static pressure was always greater than the true static pressure. The results are presented in dimensionless form as a function of the Reynolds number based on hole diameter and friction velocity. [8] Hole diameters below 0.5 mm result in large response times and the holes are easily blocked by dust in the flow. Large holes, however, are less accurate by the amount of distortion they introduce in the flow field. In reality, small holes are difficult to machine, they are exceedingly difficult to keep burr-free, and small holes are slow to respond to pressure. The shear stress of the boundary layer passing over the static pressure hole induces recirculating flows in the cavity, which in turn entrains relatively high momentum fluid from the free stream into the static pressure hole. This results in a static pressure in the passage which is higher than the pressure on the surface.

Normally for negative pressure (upper surface) manometer reading should be positive and for positive pressure (lower surface) manometer reading should be negative. But in this case for all tapping points manometer readings were positive. This occurred for the hole size that gives rise to pressure. Therefore, the whole curve shifts upwards.

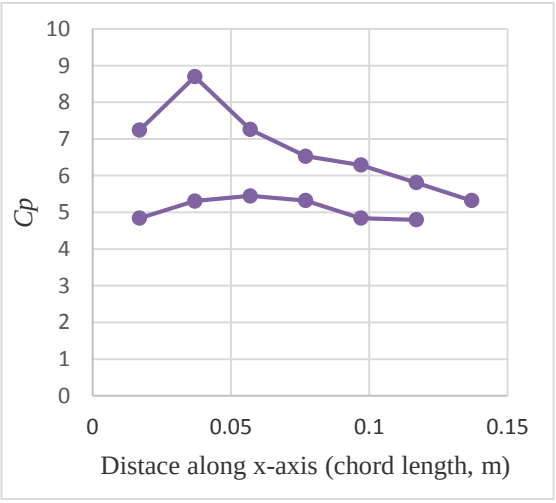

Fig.12: C_P along chord length for angle of attack 10°.

4. CONCLUSION

Aircraft design is one of the most active field that fully utilizes the laws and principles of Aerodynamics. The optimum use of both the wind tunnel testing and CFD simulation, instead of only one will help anyone to get the whole idea. The objectives of this experiment were full filled, although there are minor hiccups. This project concluded the followings:

a) The lift coefficient increases with the increase of angle of attack and becomes highest before reaching the stall angle.
b) Stall angle at given parameter was 38°.
c) Lift to drag coefficient is maximum or the performance is maximum at 6°.
d) Though lift and drag force was increasing with angle of attack but lift drag ratio began to decrease after angle 6°.

5. REFERENCES

[1] Dmitri Kuzmin, *A Guide to Numerical Methods for Transport Equation*, 2010.
[2] John D. Anderson, Jr., *Fundamentals of Aerodynamics*, 1984.
[3] http://m-selig.ae.illinois.edu/ads/afplots/naca2412.gif
[4] http://m-selig.ae.illinois.edu/ads/coord/naca2412.dat
[5] Dr. A. Sobachkin, Dr. G. Dumnov, *"Numerical Basis of CAD-Embedded CFD"*, February 2014.
[6] E.L. Houghton, *Aerodynamics for Engineering Students*, Sixth Edition.
[7] https://www.grc.nasa.gov/www/K-12/airplane/ldrat.html
[8] Shaw R (1960) "*Influence of hole dimensions on static pressure measurements"*, J. Fluid Mechanics, Vol. 7, pp. 550-564.

6. NOMENCLATURE

Symbol	Meaning	Unit
L	Lift force	(N)
D	Drag force	(N)
C_L	Co-efficient of lift	(Dimensio
C_D	Co-efficient of drag	nless.)
C_P	Co-efficient of pressure	,,